

Elastic Behavior of Zeolite Mesolite under Hydrostatic Pressure

Yongjae Lee¹, Yongmoon Lee¹, Dong-Hoon Seung¹ and Young-Nam Jang^{2*}

¹Department of Earth System Sciences, Yonsei University, Seoul 120-749, Korea

²Korea Institute of Geoscience and Mineral Resources, Daejeon, 305-350, Korea

제올라이트 메소라이트의 수압 하 탄성특성

이용재 · 이용문 · 성동훈 · 장영남*

¹연세대학교 지구시스템과학과, ²한국지질자원연구원 지구환경연구본부

제올라이트 메소라이트($\text{Na}_{5.33}\text{Ca}_{5.33}\text{Al}_{16}\text{Si}_{24}\text{O}_{80}\cdot 21.33\text{H}_2\text{O}$)에 대한 고압에서의 회절자료가 200 마이크로 크기로 단색화된 방사광가속기 X선원과 다이아몬드 앤빌셀을 사용하여 5 GPa까지 측정되었다. 물과 알코올을 사용한 수압 하에서 메소라이트의 초기 탄성 특성은 0.5 GPa에서 1.5 GPa 사이에서 일어나는 *ab*-평면의 연속적인 팽창과 *c*-축 상의 수축에 기인한 전체적인 격자부피의 팽창으로 관찰된다. 이후의 압력에서는 회절패턴의 변화로부터 질서-무질서 전이의 증거가 보여진다. 메소라이트의 *c*-축에 평행한 채널에는 양이온으로서 소듐과 칼슘이 *b*-축 방향으로 1:2 비율의 질서 있는 배열을 보이고 있는데 이로 인해 1.5 GPa까지에서는 이러한 배열의 증거인 $3b_{\text{natrolite}}$ 격자패턴이 관찰된다. 격자부피의 확장 이후 1.5 GPa 이상에서 2.5 GPa 까지에서는 격자부피 변화의 정도가 약해지며, 양이온의 무질서적인 배열에 의한 $b_{\text{natrolite}}$ 격자패턴이 관찰된다. 이후 압력의 계속된 증가는 점진적인 격자부피의 감소를 유발시키며 새로운 형태의 질서 있는 배열상을 지시하는 $3c_{\text{natrolite}}$ 격자패턴으로의 변화를 보여준다. 이로부터 압력에 의한 초수화 상태의 메소라이트는 질서-무질서-질서 형태의 채널 내부 혹은 채널간의 양이온 배열패턴 변화를 겪는 것으로 추정할 수 있다.

주요어 : 제올라이트, 메소라이트, 고압, X선 회절

Powder diffraction patterns of the zeolite mesolite ($\text{Na}_{5.33}\text{Ca}_{5.33}\text{Al}_{16}\text{Si}_{24}\text{O}_{80}\cdot 21.33\text{H}_2\text{O}$), with a natrolite framework topology were measured as a function of pressure up to 5.0 GPa using a diamond-anvil cell and a 200 μm -focused monochromatic synchrotron X-ray. Under the hydrostatic conditions mediated by pore-penetrating alcohol and water mixture, the elastic behavior of mesolite is characterized by continuous volume expansion between ca. 0.5 and 1.5 GPa, which results from expansion in the *ab*-plane and contraction along the *c*-axis. Subsequent to this anomalous behavior, changes in the powder diffraction patterns suggest possible reentrant order-disorder transition. The ordered layers of sodium- and calcium-containing channels in a 1:2 ratio along the *b*-axis attribute to the $3b_{\text{natrolite}}$ cell below 1.5 GPa. When the volume expansion is completed above 1.5 GPa, such characteristic ordering reflections disappear and the $b_{\text{natrolite}}$ cell persists with marginal volume contraction up to ca. 2.5 GPa. Further increase in pressure leads to progressive volume contraction and appears to generate another set of superlattice reflections in the $3c_{\text{natrolite}}$ cell. This suggests that mesolite in the pressure-induced hydration state experiences order-disorder-order transition involving the motions of sodium and calcium cations either through cross-channel diffusion or within the respective channels.

Key words : zeolite, mesolite, high-pressure, X-ray diffraction

1. Introduction

Mesolite belongs to the group of fibrous, small-pore zeolites with a natrolite topology (Baerlocher *et al.*, 2007). This framework is composed of T_5O_{10} building units

formed from linkages of five TO_4 tetrahedra ($\text{T}=\text{Al}, \text{Si}$). These units are then connected to form the so-called natrolite chains along the *c*-axis. The mode of linkage of the chains is such that helical 8-ring channels are formed along the *c*-axis with $\text{T}_{10}\text{O}_{20}$ windows intersecting perpendicular to these channels (Gottardi and Galli, 1985). The flexible linkages

*Corresponding author: crystal@rock25t.kigam.re.kr

between and within the chains and their interactions with charge-balancing cations and water molecules give rise to various structural distortions depending on composition, temperature, and pressure (Baur and Joswig, 1996; Baur *et al.*, 1990; Gillet *et al.*, 1996; Stahl and Hanson, 1994). Under ambient conditions, the aluminosilicate natrolite (ideal chemical composition: $\text{Na}_{16}\text{Al}_{16}\text{Si}_{24}\text{O}_{80}\cdot 16\text{H}_2\text{O}$) has an ordered distribution of Al and Si over the T-sites in *Fdd2* (orthorhombic) symmetry with sodium cations along the channels and water molecules close to the $\text{T}_{10}\text{O}_{20}$ windows. Scolecite ($\text{Ca}_8\text{Al}_{16}\text{Si}_{24}\text{O}_{80}\cdot 24\text{H}_2\text{O}$) is a natural Ca-endmember of natrolite where the substitution of all Na cations by Ca and water causes a lowering of the unit cell symmetry from orthorhombic *Fdd2* to pseudo-orthorhombic *Fd* (Kvick *et al.*, 1985). Mesolite ($\text{Na}_{5.33}\text{Ca}_{5.33}\text{Al}_{16}\text{Si}_{24}\text{O}_{80}\cdot 21.33\text{H}_2\text{O}$) is another natural analogue of natrolite where 2/3 of the Na cations in natrolite are replaced by Ca and H_2O (Artioli *et al.*, 1986). The structure of mesolite is composed of one natrolite-like and two scolecite-like layers alternating along the *b*-axis, resulting in a superlattice structure ($b_{\text{mesolite}} = 3b_{\text{natrolite}}$) with *Fdd2* symmetry and a tripling of the unit cell composition to $\text{Na}_{16}\text{Ca}_{16}\text{Al}_{48}\text{Si}_{72}\text{O}_{240}\cdot 64\text{H}_2\text{O}$ (Fig. 1). The characteristic ordering of the Na- and Ca-channels in mesolite has been known to be affected by hydrostatic pressure via pressure-induced hydration, i.e., in our previous experiment, evidence of the $3b_{\text{natrolite}}$ to $b_{\text{natrolite}}$ transition has been confirmed to occur concomitant

to pressure-induced volume expansion above 1.5 GPa (Lee *et al.*, 2002). In an attempt to get further insight on this transition, we have repeated the hydrostatic compression experiment and report here the detailed elastic behavior of mesolite using a diamond-anvil cell (DAC) and a 200 μm -focused monochromatic synchrotron X-ray beam.

2. Experimental

Mineral mesolite (Poona, India, EPMA: $\text{Na}_{4.8}\text{Ca}_{5.1}\text{Al}_{15.4}\text{Si}_{24.0}\text{O}_{80}\cdot 21.3\text{H}_2\text{O}$) was purchased from the OBG International. A modified Merrill-Bassett diamond anvil cell (DAC) was used for the high-pressure experiments, equipped with two type-I diamond anvils (culet diameter of 700 μm) and tungsten-carbide supports. A stainless-steel foil of 250 μm thickness was pre-indented to a thickness of about 100 μm , and a 250 μm hole was obtained by electro-spark erosion. A powdered sample of mesolite was placed in the gasket hole together with some ruby chips for pressure calibration (Bell and Mao, 1979). A methanol:ethanol:water (16:3:1 by volume) mixture was used as pore-penetrating hydrostatic pressure-transmitting medium in the DAC. The pressure the sample was exposed to in the DAC was measured by detecting the shift in the R1 emission line of the included ruby chips (precision: ± 0.05 GPa). The sample was equilibrated for about 10 minutes in the DAC before XRD measurement. High-pressure synchrotron X-ray powder

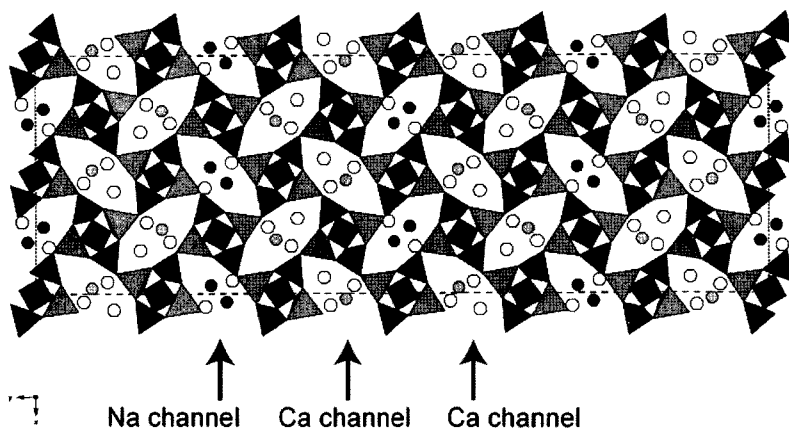


Fig. 1. A polyhedral representation of mesolite at ambient conditions viewed along [001], the chain/channel axis (structure model from Artioli *et al.*). Dark filled circles represent sodium cations, light filled ones calcium cations, and open circles water oxygen atoms. Dark (light) tetrahedra illustrate an ordered distribution of Si (Al) atoms in the framework. Dotted lines define the $3b_{\text{natrolite}}$ unit cell.

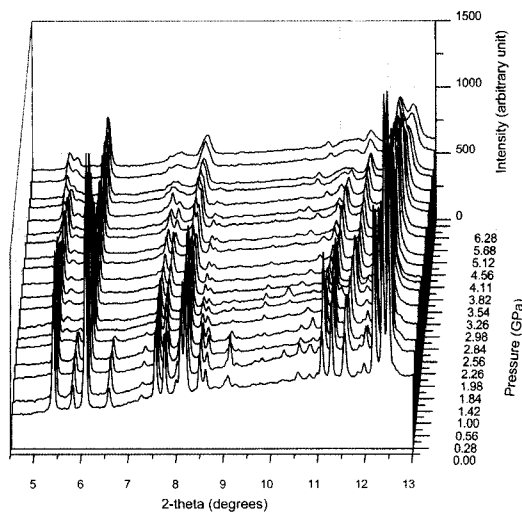


Fig. 2. Evolution of the synchrotron powder diffraction patterns of mesolite as a function of pressure (tilted view to emphasize the changes). Note the disappearance of the second reflection (i.e., $k \neq 3n$) above 1.5 GPa and splitting of the first reflection above 2.5 GPa.

diffraction measurements were performed at 5A-HFMS beamline at Pohang Accelerator Laboratory (PAL). An 18 keV synchrotron X-ray beam of 200 μm in diameter was provided by a sagittally-focusing monochromator and mirrors. Each diffraction data was measured for 1 min on MAR345 imaging plate, and the data were processed using the Fit2d suite of programs (Hammersley, 1998). Unit cell parameters were determined by whole pattern fitting using the LeBail method (Le Bail *et al.*, 1988; Toby, 2001). The diffraction peaks were modeled by varying two Gaussian and one Lorentzian parameters in the pseudo-Voigt profile function (Thompson *et al.*, 1987).

3. Results and Discussion

Changes in the powder diffraction patterns of mesolite as a function of increasing hydrostatic pressure mediated by alcohol and water mixture are shown in Fig. 2. As observed previously, the characteristic $3b_{\text{natrolite}}$ superlattice disappear around 1.5 GPa; the first three peaks indexed as (260), (111) and (131) in the $3b_{\text{natrolite}}$ cell below 1.5 GPa become (220) and (111) in the $b_{\text{natrolite}}$ cell above 1.5 GPa as the former (111) reflection disappears. Above ca. 2.5 GPa, the first peak starts to split into

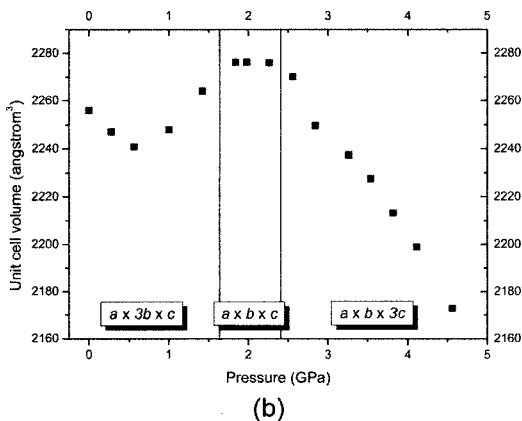
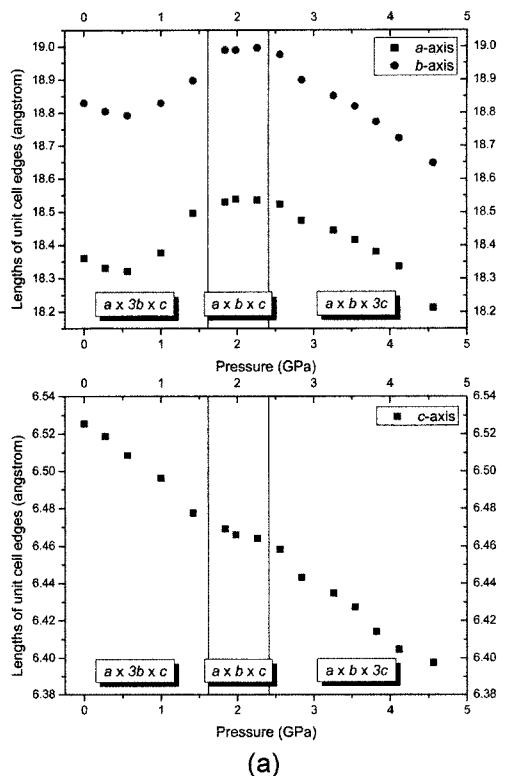


Fig. 3. (a) Changes in the unit cell edge lengths of mesolite as a function of pressure. (b) Pressure dependence of the unit cell volume of mesolite. The supercell lengths and volume are converted to respective subcell values for easier comparison. Esd's are smaller than each symbol.

two reflections and preliminary indexing of the whole pattern suggests the formation of yet another superlattice with tripled c -axis length. The resulting changes of the unit cell parameters and volume of mesolite are displayed as a function of pressure in

Fig. 3. Based on this, the elastic behavior of mesolite under hydrostatic pressure can be categorized into three regions. First below ca. 1.5 GPa, the original $3b_{\text{natrolite}}$ cell persists and exhibits initial compression followed by continuous expansion due to the 2-dimensional swelling in the *ab*-plane. This is likely the effect of pressure-induced hydration, as observed previously, but now we confirm that the volume expansion proceeds gradually unlike that observed in mineral natrolite. Upon the completion of pressure-induced volume expansion and hydration, a new phase in the $b_{\text{natrolite}}$ cell is defined between ca. 1.5 and 2.5 GPa by the absence of the superlattice reflections with $k \neq 3n$. This is an indication of an order-disorder transition of the nonframework species, i.e., sodium and calcium cations and water molecules, where the well-defined natrolite and scolecite layers become indistinguishable. During this stage, only marginal contractions in the unit cell volume as well as the cell lengths are observed. Above ca. 2.5 GPa, all the unit cell axis lengths decrease monotonically up to the final pressure of 4.6 GPa. As mentioned earlier, the disordered cell now seems to revert to another supercell by tripling the *c*-axis length. A new type of ordering of the nonframework species is envisaged to form upon this change. It would be challenging to model this phase with possibly over 400 atoms in the unit cell given the quality of the high-pressure powder diffraction data measured.

4. Conclusion

In summary, we have measured in detail the elastic behavior of zeolite mesolite under hydrostatic pressure using pore-penetrating alcohol and water mixture. We have confirmed the previously established $3b_{\text{natrolite}}$ to $b_{\text{natrolite}}$ cell transition, which we now find to occur as a result of the progressive swelling in the *ab*-plane between 0.5 and 1.5 GPa. In addition, the disordered $b_{\text{natrolite}}$ cell appears to be modulating volume contraction between 1.5 and 2.5 GPa. Above 2.5 GPa, yet another supercell with $3c_{\text{natrolite}}$ cell seems to form and persists with monotonic decrease in the elastic parameters up to 4.6 GPa. The proposed order-disorder-order transition needs to be confirmed via high-pressure single crystal diffraction studies to provide the structural details on the evolution of the nonframework species in mesolite.

Acknowledgment

This work was supported by KIGAM (Mineral Carbonation project, GP2009-002). Y. Lee and D.H Seoung thank the support from the BK21 program to the Institute of Earth, Atmosphere, and Astronomy at Yonsei University. The authors thank Dr. Hyun-Hwi Lee for the operation of 5A beam-line at PAL. Experiments at PAL were supported in part by the MEST and Pohang University of Science and Technology (POSTECH).

References

- Artioli, G., Smith, J.V. and Pluth, J.J. (1986) X-ray structure refinement of mesolite. *Acta Cryst.*, v.C42, p.937-942.
- Baerlocher, C., McCusker, L.B. and Olson, D.H. (2007) *Atlas of Zeolite Framework Types*. Elsevier, Amsterdam.
- Baur, W.H. and Joswig, W. (1996) The phases of natrolite occurring during dehydration and rehydration studied by single crystal x-ray diffraction methods between room temperature and 923K. *N. Jb. Miner. Mh.*, p.171-187.
- Baur, W.H., Kassner, D., Kim, C.-H. and Sieber, N.H. (1990) Flexibility and distortion of the framework of natrolite: crystal structures of ion-exchanged natrolites. *Eur. J. Mineral.*, v.2, p.761-769.
- Bell, P.M. and Mao, H.K. (1979) Absolute pressure measurements and their comparison with the ruby fluorescence (R1) pressure scale to 1.5 Mbar. *Carnegie Inst. Washington Year Book*, v.78, p.665-669.
- Gillet, P., Malezieux, J.-M. and Itie, J.-P. (1996) Phase changes and amorphization of zeolites at high pressures: The case of scolecite and mesolite. *Am. Mineral.*, v.81, p.651-657.
- Gottardi, G. and Galli, E. (1985) *Natural Zeolites*. Springer-Verlag, New York.
- Hammersley, A.P. (1998) FIT2D: V9.129 Reference Manual V3.1. ESRF Internal Report, ESRF98HA01T.
- Kvick, A., Stahl, K. and Smith, J.V. (1985) A neutron diffraction study of the bonding of zeolitic water in scolecite at 20K. *Z. Kristallogr.*, v.171, p.141-154.
- Le Bail, A., Duroy, H. and Fourquet, J.L. (1988) Ab-initio structure determination of LiSbWO_6 by powder x-ray diffraction. *Mat. Res. Bull.*, v.23, p.447-452.
- Lee, Y., Vogt, T., Hriljac, J.A., Parise, J.B. and Artioli, G. (2002) Pressure-Induced Volume Expansion of Zeolites in the Natrolite family. *J. Am. Chem. Soc.*, v.124, p.5466-5475.
- Stahl, K. and Hanson, J. (1994) Real-time X-ray synchrotron powder diffraction studies of the dehydration processes in scolecite and mesolite. *J. Appl. Cryst.*, v.27, p.543-550.
- Thompson, P., Cox, D.E. and Hastings, J.B. (1987) Rietveld Refinement of Dedye-Scherrer Synchrotron X-ray Data from Al_2O_3 . *J. Appl. Crystallogr.*, v.20, p.79-83.
- Toby, B.H. (2001) EXPGUI, a graphical user interface for GSAS. *J. Appl. Crystallogr.*, v.34, p.210-213.